Chaperoning of Insertion of Membrane Proteins into Lipid Bilayers by Hemifluorinated Surfactants: Application to Diphtheria Toxin†

Sergiy S. Palchevskyy,‡,§ Yevgen O. Posokhov,‡,§ Blandine Olivier,|| Jean-Luc Popot,⊥ Bernard Pucci,|| and Alexey S. Ladokhin*,‡

Department of Biochemistry and Molecular Biology, Kansas University Medical Center, Kansas City, Kansas 66160-7421, Laboratoire de Chimie Bioorganique et des Systèmes Moleculaires Vectoriels, Université d'Avignon et des Pays du Vaucluse, F-84000 Avignon, France, and Institut de Biologie Physico-Chimique, CNRS and Université Paris-7, F-75005 Paris, France

Received November 3, 2005; Revised Manuscript Received December 14, 2005

ABSTRACT: Hemifluorinated compounds, such as HF-TAC, make up a novel class of nondetergent surfactants designed to keep membrane proteins soluble under nondissociating conditions [Breyton, C., et al. (2004) *FEBS Lett. 564*, 312]. Because fluorinated and hydrogenated chains do not mix well, supramicellar concentrations of these surfactants can coexist with intact lipid vesicles. To test the ability of HF-TAC to assist proper membrane insertion of proteins, we examined its effect on the pH-triggered insertion of the diphtheria toxin T-domain. The function of the T-domain is to translocate the catalytic domain across the lipid bilayer in response to acidification of the endosome. This translocation is accompanied by the formation of a pore, which we used as a measure of activity in a vesicle leakage assay. We have also used Förster resonance energy transfer to follow the effect of HF-TAC on aggregation of aqueous and membrane-bound T-domain. Our data indicate that the pore-forming activity of the T-domain is affected by the dynamic interplay of two principal processes: productive pH-triggered membrane insertion and nonproductive aggregation of the aqueous T-domain at low pH. The presence of HF-TAC in the buffer is demonstrated to suppress aggregation in solution and ensure correct insertion and folding of the T-domain into the lipid vesicles, without solubilizing the latter. Thus, hemifluorinated surfactants stabilize the low-pH conformation of the T-domain as a water-soluble monomer while acting as low-molecular weight chaperones for its insertion into preformed lipid bilayers.

The folding and stability of membrane proteins remains one of the most elusive problems in physical biochemistry. Generally, membrane protein folding and bilayer insertion is managed by complex multiprotein assemblies, such as the endoplasmic reticulum translocon (*1*−*3*). For nonconstitutive proteins [e.g., bacterial toxins (*4*−*7*) and colicins (*8*−*10*)], however, such insertion is achieved spontaneously, in response to changes in the environment. For example, acidification of the endosome causes a conformational change in the endocytosed diphtheria toxin T-domain,[1] resulting in its insertion into the membrane and translocation of its own N-terminus with the attached catalytic domain into the cytoplasm, possibly through a pore in the lipid bilayer (*4*). Neither translocon-assisted nor spontaneous membrane insertion of proteins is well-understood on a molecular level. Despite the obvious structural and mechanistic differences between the two, recent thermodynamic evidence indicates that the underlying physicochemical principles for these processes might be the same (*11*, *12*). Thus, deciphering these principles with the help of spontaneously inserting proteins is relevant to the larger problems of membrane protein folding and stability. Recently, we have demonstrated that pH-triggered membrane insertion of the diphtheria toxin T-domain (*13*) and that of annexin B12 (*14*) are reversible processes, opening the door to their use for thermodynamic characterization of transbilayer insertion.

The principal difficulty of structural and thermodynamic studies with membrane proteins is related to their hydrophobic nature, which causes them to aggregate and precipitate outside of their native membrane environment. Solubilizing and handling them in vitro generally requires the use of dissociating surfactants (detergents). Exposing membrane proteins to detergents, however, very often makes them unstable. Several approaches have been developed in an effort to circumvent this problem (see, e.g., refs *15* and *16*), among which are transferring them to nondetergent surfac-

† This research was supported by NIH Grants GM-069783 and RR-016443 (A.S.L.). B.O. was the recipient of a doctoral fellowship from the MENESR.

* To whom correspondence should be addressed. Phone: (913) 588-0489. Fax: (913) 588-7440. E-mail: aladokhin@kumc.edu.

‡ Kansas University Medical Center.

§ These authors contributed equally to this work.

|| Université d'Avignon et des Pays du Vaucluse.

⊥ CNRS and Université Paris-7.

[1] Abbreviations: ANTS, 8-aminonaphthalene-1,3,6-trisulfonic acid; DPX, *p*-xylene-bispyridinium bromide; FRET, Förster resonance energy transfer; HF-TAC, hemifluorinated surfactant $C_2H_5C_6F_{12}C_2H_4$-S-poly-tris(hydroxymethyl)aminomethane (Figure 1A) with a critical micelle concentration (CMC) of 0.45 mM (*21*); IRF, instrument response function; LUV, extruded large unilamellar vesicles with a diameter of 100 nm; POPC, palmitoyloleoylphosphatidylcholine (from Avanti Polar Lipids); POPG, palmitoyloleoylphosphatidylglycerol (from Avanti Polar Lipids); T-domain, diphtheria toxin T-domain; T-domain-D and T-domain-A, T-domain single-cysteine mutant N235C labeled with the FRET donor dye (Alexa-532) and the acceptor dye (Alexa-647), respectively.

10.1021/bi052257l CCC: $33.50
Published on Web 02/03/2006

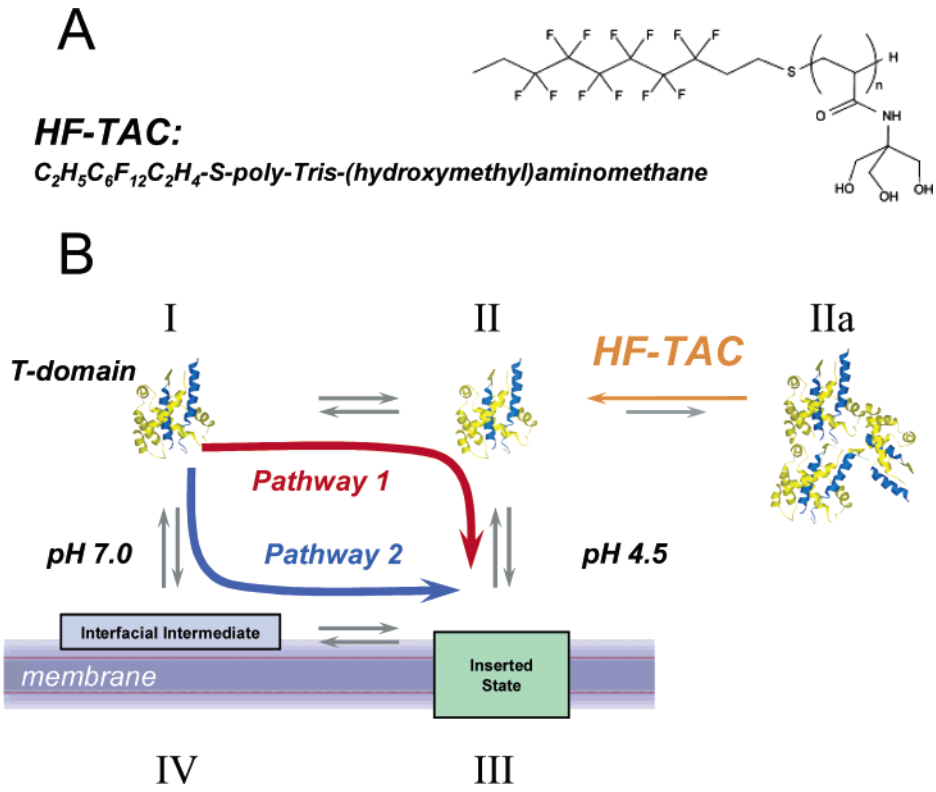

FIGURE 1: (A) Chemical structure of the hemifluorinated surfactant HF-TAC (*21*). The average degree of polymerization of the polar head of the batch used in this study was 6−7 (*n*). Because of the poor miscibility of fluorinated and hydrogenated chains, HF-TAC does not dissolve lipid bilayers even at concentrations above the CMC of 0.45 mM (cf. Figure 2). (B) Schematic representation of various conformational states of the aqueous and membranous T-domain (see the text for details). Thick red and blue arrows represent alternative insertion pathways from the solution state at neutral pH (I) to a transmembrane state at acidic pH (III). Insertion along pathway 1 is hindered by the aggregation of the T-domain in solution at low pH (IIa). Application of HF-TAC chaperones transbilayer insertion of the T-domain by suppressing nonproductive aggregation.

tants such as amphipols (*17*−*19*) or fluorinated surfactants (*20*−*22*). Hemifluorinated surfactants, in particular, present the unusual and useful combination of characteristics of being at the same time good solvents for proteins and poor solvents for lipids. These molecules, such as $C_2H_5C_6F_{12}C_2H_4$-S-poly-tris(hydroxymethyl)aminomethane (HF-TAC), are comprised of a polar head and a hydrophobic moiety that features a fluorinated central region terminated by a hydrocarbon tip (Figure 1A). The latter is designed to facilitate the adsorption of the hydrophobic chain onto protein transmembrane surfaces, which are mainly made up of methyl groups. Hemifluorinated surfactants have been shown to be able to keep several test proteins soluble, native, and stable (*22*). On the other hand, because fluorocarbons do not mix well with the hydrogenated acyl chains of the lipid, fluorinated surfactants do not solubilize membranes (they are not detergents). This opens up intriguing possibilities for the use of HF-TAC for thermodynamic studies of membrane folding and insertion of both constitutive and spontaneously inserting membrane proteins.

As a first step toward applying fluorinated surfactants to studies of membrane protein folding and stability, we have examined the effect of HF-TAC on solution properties and membrane interactions of the diphtheria toxin T-domain, which inserts into membranes under mildly acidic conditions. We have used (a) Förster resonance energy transfer (FRET) to detect aggregation of the T-domain and (b) vesicle leakage measurements to assay for T-domain transmembrane insertion and pore formation. Our data indicate that the surfactant is able to reverse aggregation of the T-domain when the membrane-competent form at acidic pH is denied a lipid environment. On the other hand, even above its critical micelle concentration (CMC), the surfactant does not prevent membrane insertion of the T-domain into the lipid bilayer. By preventing the formation of nonproductive aggregated forms of the T-domain in solution, HF-TAC promotes bilayer insertion, thus acting as a low-molecular weight chaperone [or "chemical chaperone" (*23*−*25*)] for the insertion and folding transition.

MATERIALS AND METHODS

Materials. POPC and POPG were purchased from Avanti Polar Lipids (Alabaster, AL). Alexa-532 C_5 maleimide and Alexa-647 C_2 maleimide were purchased from Molecular Probes (Eugene, OR). Two buffers, acidic and neutral, were used in this study. The acidic buffer (pH 4.5) was comprised of 10 mM sodium acetate and 50 mM NaCl, and the neutral buffer (pH 7.0) was comprised of 10 mM HEPES and 50 mM NaCl. To change the pH from 7.0 to 4.5, when necessary during the experiment, a small amount (~5% of the final volume) of a concentrated (0.5 M) acetic buffer with a pH of 4.3 was rapidly added to the sample. The final pH was confirmed in every sample using either pH-meter measurements or paper pH indicator strips. HF-TAC was synthesized as described in ref *21*. The average degree of polymerization of the polar head of the batch used in this study was 6−7 (*n*) and the average molecular weight 1520. The wild type (residues 202−378) and the single-cysteine mutant (N235C) of the diphtheria toxin T-domain were gifts from R. J. Collier.

Labeling of Single-Cysteine Mutants of the T-Domain. Labeling with Alexa dyes was performed using a standard procedure for the thiol-reactive maleimide derivatives (*26*). Typically, 1 mg of the maleimide derivative of the dye was dissolved into 0.2 mL of a 50 μM solution of protein in 10 mM HEPES (pH 7.0) containing 50 mM KCl and 1 mM EDTA. The reaction mixture was incubated overnight at 4 °C. Excess dye was removed by gel filtration chromatography (PD-10 column) followed by five consecutive centrifugations using a Microcon YM-10 concentrator, until the solution coming through the concentrator did not contain any dye, as assayed by absorbance spectroscopy. The concentration of the labeled T-domain was estimated from peak absorbance measurements, with the assumption that the extinction coefficients are the same as for the free dyes: 75 000 M^{-1} cm^{-1} for Alexa-532 and 265 000 M^{-1} cm^{-1} for Alexa-647. The protein concentration was determined spectrophotometrically using an extinction coefficient of 17 000 M^{-1} cm^{-1} at 280 nm. The labeling efficiency was estimated from the absorbance measurements at 280 nm (protein and dye) and in the maximum of the corresponding dye. The contribution of the dye at 280 nm was estimated using the absorbance of the free dye after reaction with glutathione. The labeling efficiency was found to be ~0.8, unavoidable errors associated with correcting for the relatively high absorbance of the dyes at 280 nm influencing the precision of this estimate.

Sample Preparation. Large unilamellar vesicles (LUV) with a diameter of 0.1 μm were prepared by extrusion (*27*, *28*). For leakage studies, the vesicles were preloaded with 1 mM ANTS and 10 mM DPX as described in ref *29*. Both leakage and FRET samples contained final concentrations of 0.4 μM T-domain and 3 mM lipids (1:4 POPG:POPC molar ratio) and, when present, 1 mM HF-TAC. The wild-type T-domain was used in leakage studies. We found no effect of HF-TAC or T-domain on the fluorescence properties of ANTS or on the quenching ability of DPX.

Steady-State Fluorescence Measurements. Fluorescence was measured using an SLM 8100 steady-state fluorescence spectrometer (Jobin Yvon, Edison, NJ, formerly SLM/AMINCO, Urbana, IL) equipped with double-grating excitation and single-grating emission monochromators. All experimental details for FRET measurements were exactly the same as described previously (*14*). Briefly, fluorescence excitation spectra of the dye-labeled T-domain were obtained by averaging 5−10 scans collected over a 470−660 nm range using 1-nm steps. The emission monochromator was set at 680 nm. Leakage of ANTS/DPX was followed by kinetic measurements of intensity with excitation and emission wavelengths of 353 and 520 nm, respectively.

Time-Resolved Measurements and Analysis. Fluorescence decays were measured with a FluoTime 200 time-resolved fluorescence spectrometer (PicoQuant, Berlin, Germany) using a standard time-correlated single-photon counting scheme. Samples were excited at 504 nm by a PLS 500 subnanosecond diode lamp (PicoQuant) with a repetition rate of 10 MHz. Fluorescence emission of the donor dye was detected at 550 nm via a polarizer set at 54.7°. The fluorescence intensity was recorded within 4096 channels (34 ps/channel). Data were normally collected to a constant peak value of 4000 counts. The instrumental response function (IRF) was recorded under the same conditions at the excitation wavelength by replacing the sample with a scattering solution of colloidal silica (LUDOX, Grace).

The fluorescence intensity decay was analyzed using FluoFit (PicoQuant). The program uses an iterative fitting procedure based on the Marquardt algorithm to minimize the deviation of the experimental data, presented as the sum of the exponential components:

$$I(t) = \sum_i \alpha_i e^{(-t/\tau_i)} \quad (1)$$

where α_i values are the pre-exponential amplitudes and τ_i values are the lifetimes of the decay components. Deviations from the best fit were characterized by their reduced χ^2 statistic. In addition to the χ^2 value, graphical tests such as the plot of weighted residuals were used to assess the accuracy of the fit. The number of exponentials was increased until the quality of fit did not improve.

Both steady-state and time-resolved FRET measurements were repeatedly performed after each change in sample conditions (e.g., addition of vesicles or change in pH), with increasing time intervals to cover a period of at least 24 h. The data presented here were collected after equilibrium was established, normally at least 1 h after the change in conditions, unless otherwise indicated.

RESULTS AND DISCUSSION

A general scheme for membrane interactions of the T-domain is presented in Figure 1B. The crystallographic structure (*30*) of the T-domain in the water-soluble state at neutral pH (I) provides a starting point for trying to understand the insertion process. The structure of the final transmembrane state (III) inserted at acidic pH is not known. Several topological models have been proposed, with the number of transmembrane helices varying from two to four. There seems to be little controversy, however, about the transmembrane location of the consensus insertion hairpin (highlighted in blue in the crystallographic structure in Figure 1B) comprised of H8 and H9 (*7*, *31*−*33*). Although very little is known about the structure of the recently identified (*13*) intermediate membrane state at pH 7 (IV), there is no reason to believe that it adopts a transmembrane conformation. For the sake of simplicity, a number of states suggested to exist at intermediate pH (*34*, *35*) are not shown. Importantly, the transitions between various states have been demonstrated to be reversible (*13*), which is a prerequisite for their thermodynamic characterization. The free energy of transfer from state I to IV at pH 7 is approximately −7.5 kcal/mol, which means that, under the conditions of our experiments (3 mM lipids), most of the T-domain is membrane-bound even at this pH.

Because pore formation has been associated with the action of the T-domain (*36*, *37*), we have used vesicle leakage experiments as a simplified assay for T-domain activity (Figure 2). Vesicles were loaded with the ANTS/DPX dye/quencher pair (*29*), and the kinetics of their release was monitored fluorimetrically after the vesicles were mixed with the T-domain at time zero. Zero leakage corresponds to the fluorescence level of intact LUV, while 100% leakage corresponds to the fluorescence level of LUV completely dissolved by high levels (1.5%) of reduced Triton X-100. Our data indicate that the pore-forming activity of the

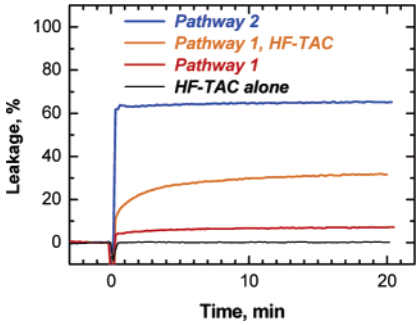

FIGURE 2: Leakage of lipid vesicle contents resulting from the membrane insertion of the T-domain was monitored as the increase in fluorescence from ANTS/DPX-loaded LUV. At time zero, the T-domain was inserted into a transmembrane conformation either by mixing it with LUV at pH 4.5 (red line, pathway 1 from Figure 1B) or by changing the pH from 7 to 4.5 in the presence of LUV (blue line, pathway 2 from Figure 1B) by adding appropriate amounts of concentrated acidic buffer. The former resulted in a loss of pore-forming activity, due to the formation of aggregates in solution (Figures 3 and 4). The presence of 1 mM HF-TAC rescues the activity of the T-domain (orange line), while HF-TAC alone at the same concentration causes no leakage (black trace).

T-domain depends strongly on the available insertion pathway. If the protein was prebound to the vesicles at neutral pH and then inserted when the pH was lowered (pathway 2, blue arrow in Figure 1B), the activity was quite high (Figure 2, blue trace). If the protein was transformed into a membrane-competent form first and then mixed with the membranes (pathway 1, red arrow in Figure 1B), the activity was markedly reduced (Figure 2, red trace), especially if the protein was incubated in state II as a concentrated stock solution (~0.2 mM) for an extended period of time (2 h in this case). This loss of pore-forming activity could possibly be due to the formation of inactive, perhaps aggregated forms of the T-domain in solution at low pH, a hypothesis that would be consistent with the observation that a larger fragment of diphtheria toxin, containing both the C- and T-domains, does undergo massive oligomerization at low pH (*38*).

We therefore examined the aggregation state of the T-domain in solution and in the presence of LUV using a FRET approach we have recently developed and used to follow changes in the oligomeric state of membrane-inserted annexin B12 (*14*) and to differentiate monomeric and oligomeric Ca^{2+}-bound forms in a family of human annexins (*39*). The single-cysteine T-domain mutant N235C was labeled with either a donor dye (D, Alexa-532) or an acceptor dye (A, Alexa-647). To minimize any structural perturbation, the labels are attached to an exposed residue between helices H2 and H3, neither of which has been suggested to insert into a transmembrane orientation in any of the published topological models (*7*, *33*). Excitation spectra were measured using samples containing a 1:2 ratio of T-domain-D and T-domain-A under various conditions. At neutral pH, the excitation spectrum of the T-domain-D/T-domain-A mixture coincided with that of the acceptor alone (Figure 3A, cyan dotted line). This indicates the absence of FRET, as is expected for a monomeric protein. Lowering the pH in the absence of membranes resulted in the appearance of a donor-associated excitation peak at 530 nm (magenta dotted line), which indicates aggregation under these conditions. While addition of LUV to the protein at neutral pH resulted in no

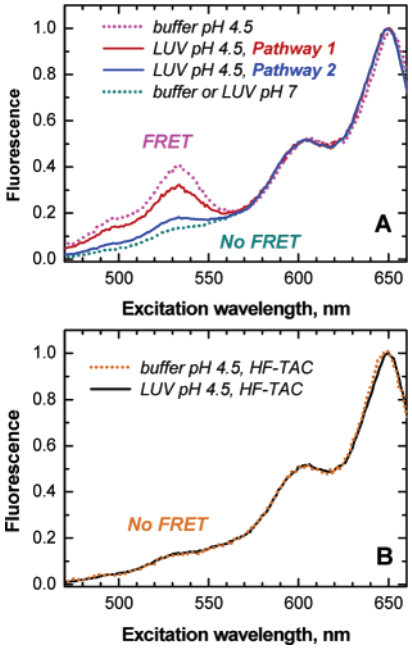

FIGURE 3: FRET-based detection of the formation of the T-domain aggregates using an experimental scheme developed in our previous study (*14*). Excitation spectra are measured for a 1:2 molar mixture of T-domain-D and T-domain-A in buffer (dotted lines) and in the presence of LUV (solid lines), in the absence (A) and presence of 1 mM HF-TAC (B). The appearance of characteristic FRET-related peaks, corresponding to the contribution of donor to the excitation spectrum measured at acceptor emission, indicates strong T-domain aggregation in buffer when the pH is changed from 7 (cyan dotted line) to 4.5 (magenta dotted line). Membrane insertion at pH 4.5 results in samples showing various degrees of aggregation depending on the insertion pathway, with stronger FRET observed for pathway 1 (red solid line) than for pathway 2 (blue solid line). The presence of 1 mM HF-TAC abolishes aggregation at low pH both in the absence (B, orange dotted line) and in the presence of LUV (black solid line).

measurable FRET (not shown), the intensity of the FRET signal in membranes at low pH was found to be pathway-dependent, being much lower for pathway 2 (Figure 3A, blue solid line) than for pathway 1 (Figure 3A, red solid line). Thus, the difference in FRET observed along the two pathways correlates with the loss of activity (Figure 2), suggesting that the inactivation of the T-domain is indeed related to aggregation.

Next we examined the effect of the hemifluorinated surfactant on the aggregation and pore-forming activity of the T-domain. The presence of 1 mM HF-TAC completely abolished the appearance of the FRET signal at low pH regardless of the presence of the vesicles or the insertion pathway (Figure 3B). The addition of surfactant not only prevented aggregation but also reversed it if the sample was first incubated at low pH and HF-TAC was subsequently added. Reversibility was detected both with steady-state excitation measurements (data similar to those in Figure 3B, but not shown) and with time-resolved measurements of donor emission (Figure 4). The fluorescence decay following a pulsed excitation measured for the T-domain-D/T-domain-A mixture at pH 7 (step 1, cyan trace) is essentially monoexponential, with a lifetime of 3.5 ns. It coincides with the decay observed for a sample containing only T-domain-D, again confirming the absence of FRET under these conditions. After incubation at pH 4.5, the decay becomes

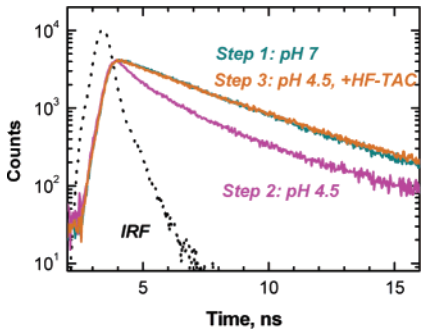

FIGURE 4: Reversibility of aggregation of the T-domain caused by addition of HF-TAC examined by measuring the changes in the fluorescence decay of the donor-labeled T-domain. Final sample concentrations were the same as for the steady-state experiment (Figure 3). Fluorescence decay kinetics (colored lines) were measured following the excitation pulse from a light-emitting diode (the IRF lamp profile is shown as a dotted line) and then fitted by multiexponential functions (see the text for parameters and other details). First, the sample containing the mixture of the donor- and acceptor-labeled T-domain was measured in buffer at pH 7 (step 1, cyan). Then the pH was lowered to 4.5 by addition of an appropriate aliquot of concentrated acetic buffer, resulting in a FRET-related shortening of the fluorescence lifetime (step 2, magenta). Addition of 1 mM HF-TAC (from a 50 mM stock) restores the original decay kinetics (step 3, orange).

heterogeneous (Figure 4, step 2, magenta trace) and can be described as the sum of a long component with a lifetime of 3.5 ns, corresponding to the monomer, and a short one with a lifetime of 1.3 ns, corresponding to aggregates. The fractional amplitudes were found to be 0.41 and 0.59 for the monomeric and aggregated component, respectively. Given the Förster distance of 60 Å for this donor/acceptor pair (*14*) and a FRET efficiency E of $1 - (1.3\ \text{ns}/3.5\ \text{ns})$ (0.63) estimated from the lifetime experiment, the average effective distance between the dyes in the aggregate is ~55 Å. This estimate was derived, of course, under very simplified assumptions, ignoring, in particular, the probable heterogeneity of the aggregated form.

FRET measurements allow us to modify the insertion scheme in Figure 1 by including an aggregated state IIa.[2] The cartoon representing this state is not meant to be structurally accurate but simply to illustrate the occurrence of aggregation. Importantly, even after an extended incubation at pH 4.5, the aggregation of the T-domain can be totally reversed by addition of HF-TAC (Figure 4, step 3, orange trace), as symbolized by the orange arrow from state IIa to II in Figure 1B.

The next question is whether the monomeric T-domain is still capable of inserting into the membranes (transition from state II to III) in the presence of a relatively high concentration of HF-TAC. This question is answered by the leakage experiment (Figure 2, orange trace), which indicates increased pore-forming activity (compare to the red trace). No leakage of vesicle content was observed upon addition of HF-TAC alone in this concentration range (Figure 2, black trace). The activity of the T-domain in the presence of HF-TAC no longer depends on the insertion pathway. The observed level of leakage, however, does not reach the level achieved by following pathway 2 in the absence of surfactant (Figure 2, blue trace). This can be explained, for example, by assuming that the T-domain is distributed between the bilayer-inserted and surfactant-bound states, which could have similar free energies. Although leakage experiments are not designed to provide thermodynamic information about membrane insertion, they clearly show that the presence of surfactants does not prevent the formation of the active membrane-inserted form. Needless to say, these experiments could not have been performed using detergents, since the membranes would have been totally disrupted long before reaching a concentration twice the CMC, as has been done here [the CMC of HF-TAC is 0.45 mM (*21*)].

An interesting possibility suggested by our data is that the pore-forming state of the T-domain might be a monomer, which is supported by two pieces of evidence: (a) a pathway-determined correlation of the reduced FRET and increased pore-forming activity of the T-domain (Figures 2 and 3A) and (b) total elimination of aggregation by HF-TAC, with preservation of the activity (Figures 2 and 3B). A much lower level of FRET is observed for the sample of the T-domain inserted into the vesicles along pathway 2 (Figure 3, blue solid line) than for that inserted along pathway 1 (Figure 3, red solid line). The residual FRET in the former case can be rationalized in principle by two alternative explanations. First, the membrane-inserted T-domain is a monomer, but because insertion does not occur with 100% efficiency even along pathway 2, a small amount of FRET is due to aggregation of a noninserted fraction. Another possibility is that all (or most) of the membrane-inserted T-domain exhibits FRET, but with an efficiency much lower than that observed in solution at low pH. The latter possibility can be ruled out, however, because it is contradicted by the total absence of FRET when the T-domain is inserted into vesicles with the help of HF-TAC (Figure 3). It is also refuted by time-resolved data indicating that the lifetime of the main fraction of the T-domain in the presence of LUV, regardless of the insertion pathway, falls in the range of 3.4−3.6 ns, which coincides with the lifetime of the monomeric T-domain at neutral pH (3.5 ns).

It has been demonstrated that the size of the solutes released by the T-domain increases with protein concentration (*40*), which is not uncommon for pore formers and is usually considered to be a hallmark of aggregation. This happens, however, at protein:lipid ratios much higher than those used in this study. The possibility that pores allowing the leakage of relatively small dyes are rather transient leakage pathways formed by several inserted helices of a monomeric T-domain cannot be ruled out. Thus, the demonstration that a monomeric T-domain causes release of dyes from vesicles does not imply that the functional state of the T-domain responsible for translocation of a catalytic domain into the cell is also a monomer. Importantly, insertion of the T-domain into a lipid bilayer as a monomer simplifies future thermodynamic analyses of insertion, because oligomerization need not be taken into account. Such an analysis

[2] The existence of aggregated form IIa affects our previous estimate of the free energy for the transmembrane insertion of the T-domain [−8 to −10 kcal/mol (*13*)]. This number can no longer be attributed solely to the II−III transition (Figure 1) but is influenced by the transition between II and IIa. This means that the true value of the free energy for the II−III transition is larger than 8−10 kcal/mol, which explains our somewhat puzzling result suggesting a relatively small difference (~2 kcal/mol) between the free energy of interfacial partitioning at neutral pH (from I to IV) and that of transmembrane insertion at acidic pH (from II to III). Determining the energetics of the aggregation, however, goes beyond the scope of this study.

in general will require a determination of the partitioning of a membrane protein between the bilayer and the surfactant under equilibrium conditions. Interestingly, another protein that inserts into the lipid bilayer in a similar fashion at low pH and forms a water-filled pore, annexin B12 (*41*), is also a monomer in its transmembrane state (*14*).

Taken together, our FRET and pore formation experiments indicate that the efficiency of membrane insertion of the T-domain is pathway-dependent and affected by nonproductive aggregation at low pH. HF-TAC suppresses aggregation in solution and, by doing so, facilitates the correct insertion and folding of the T-domain into lipid vesicles. Nondetergent surfactants such as hemifluorinated surfactants (this work) or amphipols (*42*) thus have this interesting potential to deliver solubilized membrane proteins to preformed lipid bilayers without dissolving the latter as a detergent would do. In so doing, they effectively play the role of low-molecular weight (or chemical) chaperones. Fluorinated surfactants appear to be particularly promising for studies of membrane protein insertion, inasmuch as they permit, in principle, investigations of the structure of intermediates (e.g., the low-pH-activated form of the T-domain in solution) and of the conformational changes and energetics of insertion to be carried out under equilibrium conditions.

ACKNOWLEDGMENT

We are grateful to Dr. R. John Collier for his gift of the T-domain.

REFERENCES

1. Johnson, A. E., and van Waes, M. A. (1999) The translocon: A dynamic gateway at the ER membrane, *Annu. Rev. Cell Dev. Biol. 15*, 799−842.
2. Alder, N. N., and Johnson, A. E. (2004) Cotranslational membrane protein biogenesis at the endoplasmic reticulum, *J. Biol. Chem. 279*, 22787−22790.
3. Rapoport, T. A., Goder, V., Heinrich, S. U., and Matlack, K. E. S. (2004) Membrane-protein integration and the role of the translocation channel, *Trends Cell Biol. 14*, 568−575.
4. Oh, K. J., Senzel, L., Collier, R. J., and Finkelstein, A. (1999) Translocation of the catalytic domain of diphtheria toxin across planar phospholipid bilayers by its own T domain, *Proc. Natl. Acad. Sci. U.S.A. 96*, 8467−8470.
5. Miller, C. J., Elliott, J. L., and Collier, R. J. (1999) Anthrax protective antigen: Prepore-to-pore conversion, *Biochemistry 38*, 10432−10441.
6. Shatursky, O., Heuck, A. P., Shepard, L. A., Rossjohn, J., Parker, M. W., Johnson, A. E., and Tweten, R. K. (1999) The mechanism of membrane insertion for a cholesterol-dependent cytolysin: A novel paradigm for pore-forming toxins, *Cell 99*, 293−299.
7. Senzel, L., Gordon, M., Blaustein, R. O., Oh, K. J., Collier, R. J., and Finkelstein, A. (2000) Topography of diphtheria toxin's T domain in the open channel state, *J. Gen. Physiol. 115*, 421−434.
8. Zakharov, S. D., Lindeberg, M., and Cramer, W. A. (1999) Kinetic description of structural changes linked to membrane import of the colicin E1 channel protein, *Biochemistry 38*, 11325−11332.
9. Tory, M. C., and Merrill, A. R. (1999) Adventures in membrane protein topology: A study of the membrane-bound state of colicin E1, *J. Biol. Chem. 274*, 24539−24549.
10. Parker, M. W., Tucker, A. D., Tsernoglou, D., and Pattus, F. (1990) Insights into membrane insertion based on studies of colicins, *Trends Biochem. Sci. 15*, 126−129.
11. Hessa, T., Kim, H., Bihlmaler, K., Lundin, C., Boekel, J., Andersson, H., Nilsson, I., White, S. H., and von Heijne, G. (2005) Recognition of transmembrane helices by the endoplasmic reticulum translocon, *Nature 433*, 377−381.
12. Bowie, J. U. (2005) Border crossing, *Nature 433*, 367−369.
13. Ladokhin, A. S., Legmann, R., Collier, R. J., and White, S. H. (2004) Reversible refolding of the diphtheria toxin T-domain on lipid membranes, *Biochemistry 43*, 7451−7458.
14. Ladokhin, A. S., and Haigler, H. T. (2005) Reversible transition between the surface trimer and membrane-inserted monomer of annexin 12, *Biochemistry 44*, 3402−3409.
15. Bowie, J. U. (2001) Stabilizing membrane proteins, *Curr. Opin. Struct. Biol. 11*, 397−402.
16. Gohon, Y., and Popot, J.-L. (2003) Membrane protein-surfactant complexes, *Curr. Opin. Colloid Interface Sci. 8*, 15−22.
17. Popot, J.-L., Berry, E. A., Charvolin, D., Creuzenet, C., Ebel, C., Engelman, D. M., Flötenmeyer, M., Giusti, F., Gohon, Y., Hervé, P., Hong, Q., Lakey, J. H., Leonard, K., Shuman, H. A., Timmins, P., Warschawski, D. E., Zito, F., Zoonens, M., Pucci, B., and Tribet, C. (2003) Amphipols: Polymeric surfactants for membrane biology research, *Cell. Mol. Life Sci. 60*, 1559−1574.
18. Tribet, C., Audebert, R., and Popot, J.-L. (1996) Amphipols: Polymers that keep membrane proteins soluble in aqueous solutions, *Proc. Natl. Acad. Sci. U.S.A. 93*, 15047−15050.
19. Sanders, C. R., Kuhn Hoffmann, A., Gray, D. N., Keyes, M. H., and Ellis, C. D. (2004) French swimwear for membrane proteins, *ChemBioChem 5*, 423−426.
20. Chabaud, E., Barthelemy, P., Mora, N., Popot, J.-L., and Pucci, B. (1998) Stabilization of integral membrane proteins in aqueous solution using fluorinated surfactants, *Biochimie 80*, 515−530.
21. Barthelemy, P., Ameduri, B., Chabaud, E., Popot, J.-L., and Pucci, B. (1999) Synthesis and preliminary assessments of ethyl-terminated perfluoroalkyl nonionic surfactants derived from tris-(hydroxymethyl)acrylamidomethane, *Org. Lett. 1*, 1689−1692.
22. Breyton, C., Chabaud, E., Chaudier, Y., Pucci, B., and Popot, J.-L. (2004) Hemifluorinated surfactants: A non-dissociating environment for handling membrane proteins in aqueous solutions? *FEBS Lett. 564*, 312−318.
23. Sanders, C. R., and Myers, J. K. (2004) Disease-related misassembly of membrane proteins, *Annu. Rev. Biophys. Biomol. Struct. 33*, 25−51.
24. Gelman, M. S., and Kopito, R. R. (2002) Rescuing protein conformation: Prospects for pharmacological therapy in cystic fibrosis, *J. Clin. Invest. 110*, 1591−1597.
25. Loo, T. W., and Clarke, D. M. (2003) Application of chemical chaperones to the rescue of folding defects, *Methods Mol. Biol. 232*, 231−243.
26. Haugland, R. P. (1996) *Handbook of Fluorescent Probes and Research Chemicals*, 6th ed., Molecular Probes, Inc., Eugene, OR.
27. Mayer, L. D., Hope, M. J., and Cullis, P. R. (1986) Vesicles of variable sizes produced by a rapid extrusion procedure, *Biochim. Biophys. Acta 858*, 161−168.
28. Hope, M. J., Bally, M. B., Mayer, L. D., Janoff, A. S., and Cullis, P. R. (1986) Generation of multilamellar and unilamellar phospholipid vesicles, *Chem. Phys. Lipids 40*, 89−107.
29. Ladokhin, A. S., Wimley, W. C., Hristova, K., and White, S. H. (1997) Mechanism of leakage of contents of membrane vesicles determined by fluorescence requenching, *Methods Enzymol. 278*, 474−486.
30. Weiss, M. S., Blanke, S. R., Collier, R. J., and Eisenberg, D. (1995) Structure of the isolated catalytic domain of diphtheria toxin, *Biochemistry 34*, 773−781.
31. Oh, K. J., Zhan, H., Cui, C., Hideg, K., Collier, R. J., and Hubbell, W. L. (1996) Organization of diphtheria toxin T domain in bilayers: A site-directed spin labeling study, *Science 273*, 810−812.
32. Oh, K. J., Zhan, H., Cui, C., Altenbach, C., Hubbell, W. L., and Collier, R. J. (1999) Conformation of the diphtheria toxin T domain in membranes: A site-directed spin-labeling study of the TH8 helix and TL5 loop, *Biochemistry 38*, 10336−10343.
33. Rosconi, M. P., Zhao, G., and London, E. (2004) Analyzing topography of membrane-inserted diphtheria toxin T domain using BODIPY-streptavidin: At low pH, helices 8 and 9 form a transmembrane hairpin but helices 5−7 form stable nonclassical inserted segments on the cis side of the bilayer, *Biochemistry 43*, 9127−9139.
34. Wang, Y., Malenbaum, S. E., Kachel, K., Zhan, H. J., Collier, R. J., and London, E. (1997) Identification of shallow and deep membrane-penetrating forms of diphtheria toxin T domain that are regulated by protein concentration and bilayer width, *J. Biol. Chem. 272*, 25091−25098.
35. Chenal, A., Savarin, P., Nizard, P., Guillain, F., Gillet, D., and Forge, V. (2002) Membrane protein insertion regulated by bringing

electrostatic and hydrophobic interactions into play. A case study with the translocation domain of the diphtheria toxin, *J. Biol. Chem. 277*, 43425−43432.
36. Hoch, D. H., Romero-Mira, M., Ehrlich, B. E., Finkelstein, A., DasGupta, B. R., and Simpson, L. L. (1985) Channels formed by botulinum, tetanus, and diphtheria toxins in planar lipid bilayers: Relevance to translocation of proteins, *Proc. Natl. Acad. Sci. U.S.A. 82*, 1692−1696.
37. Silverman, J. A., Mindell, J. A., Finkelstein, A., Shen, W. H., and Collier, R. J. (1994) Mutational analysis of the helical hairpin region of diphtheria toxin transmembrane domain, *J. Biol. Chem. 269*, 22524−22532.
38. Bell, C. E., Poon, P. H., Schumaker, V. N., and Eisenberg, D. (1997) Oligomerization of a 45 kilodalton fragment of diphtheria toxin at pH 5.0 to a molecule of 20−24 subunits, *Biochemistry 36*, 15201−15207.
39. Patel, D. R., Isas, J. M., Ladokhin, A. S., Jao, C. C., Kim, Y. E., Kirsch, T., Langen, R., and Haigler, H. T. (2005) The conserved core domains of annexins A1, A2, A5, and B12 can be divided into two groups with different Ca^{2+}-dependent membrane-binding properties, *Biochemistry 44*, 2833−2844.
40. Sharpe, J. C., and London, E. (1999) Diphtheria toxin forms pores of different sizes depending on its concentration in membranes: Probable relationship to oligomerization, *J. Membr. Biol. 171*, 209−221.
41. Langen, R., Isas, J. M., Hubbell, W. L., and Haigler, H. T. (1998) A transmembrane form of annexin XII detected by site-directed spin labeling, *Proc. Natl. Acad. Sci. U.S.A. 95*, 14060−14065.
42. Nagy, J. K., Kuhn Hoffmann, A., Keyes, M. H., Gray, D. N., Oxenoid, K., and Sanders, C. R. (2001) Use of amphipathic polymers to deliver a membrane protein to lipid bilayers, *FEBS Lett. 501*, 115−120.

BI052257L